Antonio Ramos
Editor

International Centre
for Mechanical Sciences

Electrokinetics and Electrohydrodynamics in Microsystems

CISM Courses and Lectures, vol. 530

SpringerWienNewYork

SpringerWienNewYork

CISM COURSES AND LECTURES

The series presents lecture notes, monographs, edited works and proceedings in the field of Mechanics, Engineering, Computer Science and Applied Mathematics.
Purpose of the series is to make known in the international scientific and technical community results obtained in some of the activities organized by CISM, the International Centre for Mechanical Sciences.

INTERNATIONAL CENTRE FOR MECHANICAL SCIENCES

COURSES AND LECTURES - No. 530

ELECTROKINETICS AND ELECTROHYDRODYNAMICS IN MICROSYSTEMS

EDITED BY

ANTONIO RAMOS
UNIVERSITY OF SEVILLE, SPAIN

SpringerWienNewYork

This volume contains 143 illustrations

Printed in Italy
SPIN 80073444

All contributions have been typeset by the authors.

ISBN 978-3-7091-0899-4 SpringerWienNewYork

PREFACE

The manipulation of colloidal particles and fluids in microsystems by using electrical forces has many existing and potential applications. The electrical manipulation at the micrometre scale presents the advantages of voltage-based control and dominance over other forces. The latter is a clear example of the scaling laws of physical systems: in the range above a few millimetres the electrical forces are rather ineffective, but in the micrometre (and submicrometre) scale the electrical forces dominate.

The present book contains the Lecture Notes of a CISM Advanced School on "Electrokinetics and Electrohydrodynamics in Microsystems", held in Udine, Italy, on 22nd-26th June 2009. The aim of the book is to provide a state-of-the-art knowledge on both theoretical and applied aspects of the electrical manipulation of colloidal particles and fluids in microsystems. The book covers the following topics: Dielectrophoresis (DEP), Electrowetting, Electrohydrodynamics (EHD) in microsystems, and Electrokinetics of fluids and particles.

The first three chapters of this book are dedicated to Dielectrophoresis. Chapter I, by Tao Sun and Hywel Morgan, presents an overview of the basis of Dielectrophoresis and its applications for the manipulation and characterization of particles. Chapters II and III, by Nicolas G. Green, examine in depth the theory of Dielectrophoresis. Chapter II provides the basics of Quasi-electrostatics from the perspective of Dielectrophoresis and Chapter III discusses the forces produced by the interaction of electric fields with the induced dipole moments on particles.

Chapter IV, by Pablo García-Sánchez and Frieder Mugele, is dedicated to Electrowetting, where fluid handling is achieved by subdividing the liquid into discrete droplets that are manipulated by electrical forces. The chapter introduces briefly basic concepts of wetting and discusses in detail the fundamental physics behind the electrowetting phenomenon. The second part of the chapter reviews applications of Electrowetting in Lab-on-Chip, Optics, displays and microfluidic devices.

Chapter V, by Antonio Ramos, provides an overview of Electrohydrodynamic pumping in microsystems. The chapter presents first the basic equations of Electrohydrodynamics in the micrometre scale.

Subsequently, five different EHD micropumps are studied and compared: from those that employ forces in the liquid bulk to those that employ forces in the electrical double layer.

Chapter VI, by Chuan-Hua Chen, is devoted to Electrohydrodynamic Stability in the context of the ohmic model. Many EHD systems, such as leaky dielectric liquids or electrolytic solutions, fall into the ohmic regime. The chapter presents first a derivation of the EHD equations in the ohmic regime. Afterwards, basic concepts of EHD stability are illustrated using two model problems: the electrokinetic mixing flow and the EHD cone-jet flow.

The last chapter of the book covers an important part of electromicrofluidics: fluid flows generated by electrical forces in the double layer. Chapter VII, by Martin Z. Bazant, presents an introduction to Induced Charge Electrokinetic (ICEK) Phenomena, where the applied electric field acts on its own induced-charge in an electrolytic solution near a polarizable surface. The chapter discusses the basic physics behind ICEK of colloidal particles (induced charge electrophoresis) and fluids (induced charge electroosmosis).

I would like to take this opportunity to thank all the contributors to this book for their valuable time and the excellence of their work. My sincere thanks are also extended to Prof. Giulio Maier, rector of CISM, to Prof. Paolo Serafini for his help in the editorial work, and to all the CISM staff in Udine. Finally, I would like to acknowledge the help of my colleagues at the University of Seville, Antonio Castellanos, Alberto T. Pérez and Antonio González, in the process of preparing both the CISM course and this book.

Antonio Ramos

CONTENTS

AC Electrokinetic Micro- and Nano-particle Manipulation and Characterization

Tao Sun and Hywel Morgan

School of Electronics and Computer Science
University of Southampton, SO17 1BJ, UK

Abstract Automated or remote manipulation and characterization of particles is a key element in microfluidic devices. Microelectrodes integrated into microfluidic devices can generate large electric fields and field gradients using low voltages. The field gradients can be used to actively drive the motion of particles by dielectrophoresis. In this chapter, the basis of AC electrokinetics is reviewed and example applications for manipulation and characterization of particles are provided.

1 Introduction

Microfluidics involves the manipulation of fluids and particles within a microscale chip. Physical parameters that characterize microfluidics include Reynolds number, diffusion, fluidic resistance, surface area to volume ratio and surface tension (Beebe et al., 2002; Stone et al., 2004). Within microfluidic systems, the manipulation of particles is of fundamental importance in bioanalytical science and biotechnology. Manipulation involves a range of processes including patterning, focusing, sorting, trapping, handling and separation. These operations call on a wide range of techniques such as hydrodynamic focusing (Lee et al., 2001; Rodriguez-Trujillo et al., 2007), electrophoresis (Lacher et al., 2001; Kremser et al., 2004), optical tweezer (Ashkin et al., 1986; Ashkin, 1997), acoustic standing waves (Wiklund et al., 2006; Laurell et al., 2007), magnetism (Pamme, 2006) and AC electrokinetics (Pohl, 1978; Pethig, 1979; Morgan and Green, 2003). Characterization of particles within microfluidic systems provides a quantitative and analytical approach to interrogate the physico-chemical properties of particles, such as size, permittivity and conductivity. In terms of cell handling a number of different methods can be combined to produce a complex technological platform. In this chapter, we describe AC electrokinetic principles and techniques whereby electric fields are used to manipulate and characterize

particles. We show how a combination of electric fields and hydrodynamics can be used to manipulate particles. The main focus of the chapter is devoted to explaining the principles and applications of dielectrophoresis (DEP). Examples of applications of various AC electrokinetic techniques are given, including a short overview of single cell impedance analysis methods.

2 AC electrokinetics

AC electrokinetics describes the general behavior of polarisable particles in an AC electric field.

2.1 Polarized Particle

If a homogeneous solid dielectric sphere (for example a solid particle with a radius of R) sits in a homogeneous dielectric medium, charges will accumulate at the interface between the particle and the medium. When an electric field is applied, positive and negative charges are pulled in opposite directions, which gives rise to an effective or induced dipole moment across the particle. The mechanism of the formation of this induced dipole, $\mathbf{p}$, is the first approximation for a polarized particle in an electric field, called the dipole approximation. The net force, $\mathbf{F}$, and torque, Γ on this polarized particle can be calculated from the induced dipole moment, and these are given by:

$$\mathbf{F} = \mathbf{p} \cdot \nabla \mathbf{E} \tag{1}$$

$$\Gamma = \mathbf{p} \times \mathbf{E} \tag{2}$$

The operator $\cdot$ is the dot product; the operator $\times$ the cross product, and ∇ the gradient of (the field). If the electric field is uniform, the net force on the dipole (particle) is zero. For a dipole at some random orientation to the field, the torque will tend to align the dipole (particle) with the electric field.

To quantitatively calculate the effective dipole moment, analysis is performed using spherical coordinates $\{r \geq 0, 0 \leq \theta \leq \pi, 0 \leq \vartheta \leq 2\pi\}$ with the particle located in a homogeneous and parallel electric field along the negative z-axis, as shown in figure 1.

The potential distributions inside the particle ϕ_p and in the medium ϕ_m are given by (Lorrain et al. 1988):

$$\phi_p = -\left(\frac{3\tilde{\epsilon}_m}{\tilde{\epsilon}_p + 2\tilde{\epsilon}_m}\right) E_0 \cos\theta \tag{3}$$

$$\phi_m = -\left[1 - \frac{R^3}{r^3}\left(\frac{\tilde{\epsilon}_p - \tilde{\epsilon}_m}{\tilde{\epsilon}_p + 2\tilde{\epsilon}_m}\right)\right] E_0 \cos\theta \tag{4}$$

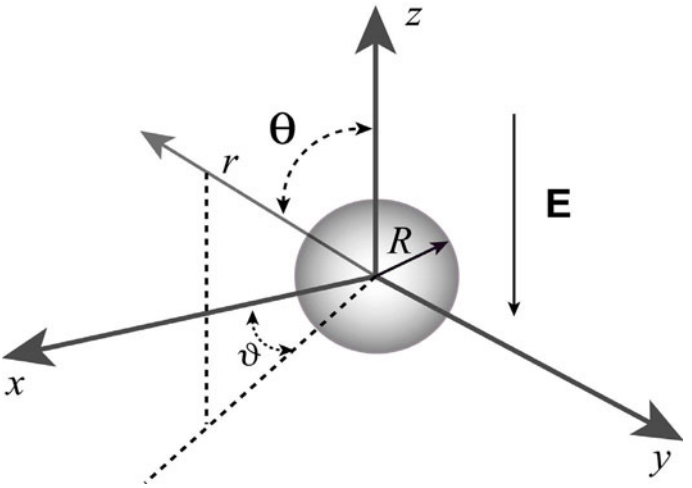

Figure 1. Diagram showing a spherical particle locating in an homogeneous and parallel electric field along with the z-axis.

where $\tilde{\epsilon} = \epsilon - j\sigma/\omega$ is the complex permittivity, $j^2 = -1$ and ω is the angular frequency. The subscripts p and m refer to particle and medium respectively. E_0 is the amplitude of the applied electric field.

The potential of the effective dipole moment $\mathbf{P}_{eff}$ can be considered as an increment in the potential distribution of the applied field, with $\mathbf{P}_{eff}$ given by:

$$\mathbf{P}_{eff} = 4\pi\tilde{\epsilon}_m \left(\frac{\tilde{\epsilon}_p - \tilde{\epsilon}_m}{\tilde{\epsilon}_p + 2\tilde{\epsilon}_m} \right) R^3 \mathbf{E} \tag{5}$$

According to equation 5, the effective dipole moment is frequency-dependent where the dependence is characterized by the Clausius-Mossotti factor $\tilde{f}_{CM}$:

$$\tilde{f}_{CM} = \frac{\tilde{\epsilon}_p - \tilde{\epsilon}_m}{\tilde{\epsilon}_p + 2\tilde{\epsilon}_m} \tag{6}$$

The Clausius-Mossotti factor provides a quantitative evaluation of the polarisability of the particle and the suspending medium. If the particle is not solid, e.g. has a shell like a cell, as shown in figure 2a then the particle complex permittivity $\tilde{\epsilon}_p$ is a function of the dielectric properties of the shell

(membrane) and the inside (cytoplasm). This is given by:

$$\tilde{\epsilon}_p = \tilde{\epsilon}_{mem} \frac{\gamma^3 + 2\dfrac{\tilde{\epsilon}_i - \tilde{\epsilon}_{mem}}{\tilde{\epsilon}_i + 2\tilde{\epsilon}_{mem}}}{\gamma^3 - \dfrac{\tilde{\epsilon}_i - \tilde{\epsilon}_{mem}}{\tilde{\epsilon}_i + 2\tilde{\epsilon}_{mem}}} \qquad \text{with}\, \gamma = \frac{R_i + d}{R_i} \tag{7}$$

where $\tilde{\epsilon}_{mem}$ is the complex permittivity of the membrane, $\tilde{\epsilon}_i$ the internal properties, and the cell has inner radius R_i and membrane thickness d.

For a cell in suspension, the dielectric properties of the suspending system has two intrinsic relaxation frequencies. The first relaxation occurs at low frequencies and is due to (Maxwell-Wagner) polarization of the cell membrane-suspending medium interface. The second relaxation, occurs at higher frequencies, and is due to polarization between the suspending medium and the cell cytoplasm, where the cell membrane capacitance is in effect short-circuited.

Figure 2b shows these two relaxations as the real and imaginary parts of the Clausius-Mossotti factor of a cell suspended in a medium with different conductivities (see legends for details). It clearly shows that the imaginary part has two peaks, each corresponding to the two relaxations.

2.2 Dielectrophoresis

The phenomenon of DEP originates from the interaction of the induced dipole moment with the applied electric field. In a field gradient there is a net force on the polarized particle that causes it to move towards either the high or low electric field regions depending on the particle (and suspending medium) properties. According to equation 1, two conditions must be satisfied for DEP to occur. First there must be a difference between the polarisability of the particle and medium so that an induced dipole moment is established across the particle. Secondly, the electric field must be non-uniform. Figure 3 shows the field configuration when a particle sits in a non-uniform electric field depending on the particle polarisability. When the particle polarisability is greater than the suspending medium, the particle behaves as a conductor and the electric field vectors bend towards the particle, meeting the surface at right angles. The field inside the particle is nearly zero, as shown in figure 3a. The converse is shown in figure 3b, where the particle polarisability is less than the medium. The field vectors now bend around the particle as if it were an insulator. When the polarisability of the particle and electrolyte are the same it is as if the particle does not exist and the field lines are parallel and continuous everywhere. The imbalance of forces on the induced dipole gives rise to particle movement, i.e. DEP. When the polarisability of the particle is greater than its surrounding

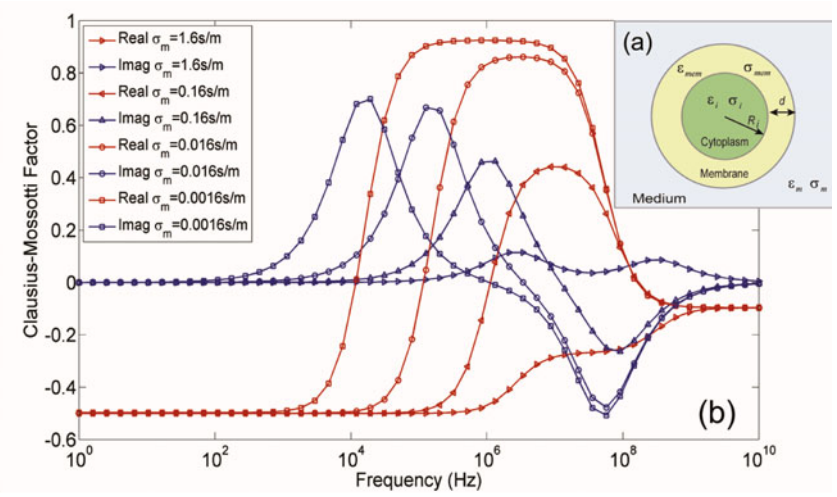

Figure 2. (a) Diagram showing a single shell spherical particle, representing a cell in suspension. (b) Plot showing a spectrum of the real and imaginary parts of the Clausius-Mossotti factor for a particle in an electrolyte, calculated for different suspending medium conductivities. The following parameters were used: $\epsilon_o = 8.854 \times 10^{-12}\,\mathrm{Fm}^{-1}$, $R_i = 3 \times 10^{-6}$ m, $d = 5 \times 10^{-9}$ m, $\epsilon_m = 80\epsilon_o$, $\epsilon_{mem} = 5\epsilon_o$, $\sigma_{mem} = 10^{-8}\,\mathrm{Sm}^{-1}$, $\epsilon_i = 60\epsilon_o, \sigma_i = 0.4\,\mathrm{Sm}^{-1}$.

medium, the direction of the dipole is with the field and the particle experiences a positive DEP force (pDEP); the particle moves towards the high field region. The opposite situation gives rise to negative DEP (nDEP); and the particle moves away from regions of high electric fields.

The time-averaged dielectrophoretic force on the dipole is given by:

$$\langle \mathbf{F}_{DEP} \rangle = \frac{1}{2}\mathrm{Re}\left[(\tilde{\mathbf{p}} \cdot \nabla)\tilde{\mathbf{E}}^*\right] = \frac{1}{2}\upsilon \mathrm{Re}\left[\tilde{\alpha}(\mathbf{E} \cdot \nabla)\tilde{\mathbf{E}}^*\right] \tag{8}$$

where $\tilde{\mathbf{p}}$ is the induced dipole moment phasor, υ the volume of the particle, $\tilde{\alpha}$ the effective polarisability and $*$ indicates complex conjugate.

If the non-uniform electric field has no spatially dependent phase, the dielectrophoretic force simplifies to:

$$\langle \mathbf{F}_{DEP} \rangle = \frac{1}{4}\upsilon \mathrm{Re}\left[\tilde{\alpha}\right] \nabla|\tilde{\mathbf{E}}|^2 \tag{9}$$

For a spherical particle, equation 9 becomes:

$$\langle \mathbf{F}_{DEP} \rangle = \pi\epsilon_m R^3 \mathrm{Re}\left[\tilde{f}_{CM}\right] \nabla|\tilde{\mathbf{E}}|^2 \tag{10}$$

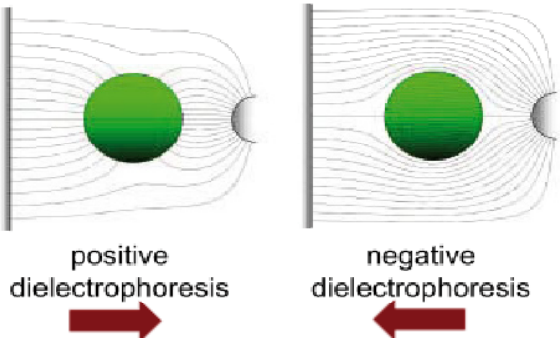

Figure 3. Diagram showing the principle of dielectrophoresis (DEP), which only occurs in a non-homogeneous electric field. (a) particle more polarizable than the medium; positive dielectrophoresis (pDEP) (b) particle less polarizable than the medium; negative dielectrophoresis (nDEP).

According to equation 10, if the electric field is uniform, the gradient of the magnitude of the field is zero ($\nabla|\tilde{\mathbf{E}}|^2 = 0$), which means that there is no DEP force. The frequency dependence and the direction of the DEP force are governed by the real part of the Clausius-Mossotti factor. If the particle is more polarisable than the medium, ($\mathrm{Re}\left[\tilde{f}_{CM}\right] > 0$), the particle is attracted to high intensity electric field regions (pDEP). Conversely, if the particle is less polarisable than the medium, ($\mathrm{Re}\left[\tilde{f}_{CM}\right] < 0$), the particle is repelled from high intensity field regions (nDEP).

2.3 Travelling wave dielectrophoresis

Note that the simplification of equation 8 to equation 9 is based on the assumption that the non-uniform electric field has no spatially dependent phase. In contrast, in electric fields with spatially varying phases, equation 8 can be expanded as:

$$\langle \mathbf{F}_{DEP} \rangle = \frac{1}{4} \upsilon \mathrm{Re}\left[\tilde{\alpha}\right] \nabla|\tilde{\mathbf{E}}|^2 - \frac{1}{2} \upsilon \mathrm{Im}\left(\nabla \times (\mathrm{Re}[\tilde{\mathbf{E}}] \times \mathrm{Im}[\tilde{\mathbf{E}}])\right) \qquad (11)$$

Equation 11 shows that the dielectrophoretic force consists of two components; the first term on the right is the DEP force; the second term is called the travelling wave DEP (twDEP) force. In this case a field with spatially varying phase can be generated with a travelling electric field as shown in

figure 4 for an interdigitated electrode array energized with a four phase AC signal. This twDEP force propels a particle along the electrode array. If there is no spatially varying phase, the imaginary part of the electric field is zero ($\mathrm{Im}[\tilde{\mathbf{E}}] = 0$), which means that there is no twDEP. In order for twDEP to be effective, the frequency of the excitation voltage and the conductivity of the medium should be chosen to satisfy two conditions: (a) the particle must experience nDEP so that it can be levitated above the electrode array and (b) the imaginary part of the Clausius-Mossotti factor has to be non-zero.

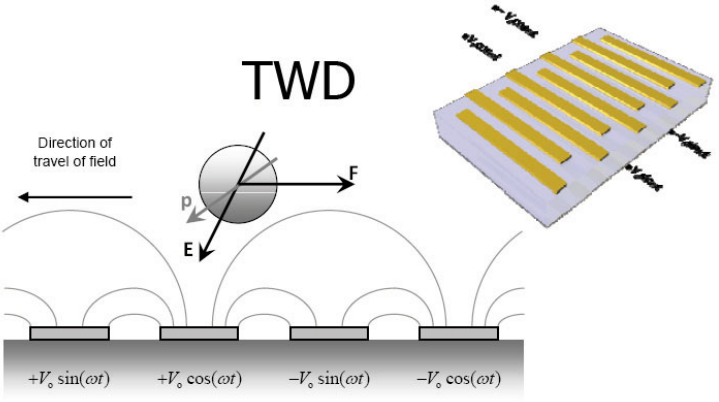

Figure 4. Diagram showing the principle of travelling wave DEP (twDEP). The consecutive phase-shifted signals generate a travelling electric field.

2.4 Electrorotation

When a dipole sits in a field, the interaction between the electric field and this dipole moment leads to a torque on the particle. There is a finite time (or phase delay) between the application of the electric field and the establishment of the dipole moment. If the field vector now changes direction, the vector of the dipole moment will try to follow the changing of field vector. If the field vector rotates then the particle will also rotate. The time-averaged rotating torque is given by:

$$\langle \mathbf{\Gamma}_{ROT} \rangle = \frac{1}{2}\mathrm{Re}\left[\tilde{\mathbf{p}} \times \tilde{\mathbf{E}}^{*}\right] = -\upsilon \mathrm{Im}[\tilde{\alpha}]\left(\mathrm{Re}[\tilde{\mathbf{E}}] \times \mathrm{Im}[\tilde{\mathbf{E}}]\right) \tag{12}$$

For a spherical particle, this becomes:

$$\langle \Gamma_{ROT} \rangle = -4\pi\epsilon_m R^3 \mathrm{Im}[\tilde{f}_{CM}]|\tilde{\mathbf{E}}|^2 \tag{13}$$

Equation 13 shows that the frequency-dependent property of the ROT torque depends on the imaginary part of the Clausius-Mossotti factor. The particle will rotate with or against the electric field, depending on whether the imaginary part of the Clausius-Mossotti factor is negative or positive. If the charge relaxation time constant of the particle is smaller than that of the medium ($\tau_p = \epsilon_p/\sigma_p < \tau_m = \epsilon_m/\sigma_m$), the particle rotates with the changing direction of the field. If $\tau_m < \tau_p$, the particle rotates against the field. In a viscous medium, the particle rotates at a constant angular velocity. The ROT torque can be measured indirectly by analysis of this angular velocity, which is given by (Arnold and Zimmerman 1988)

$$R_{ROT}(\omega) = -\frac{\epsilon_m \mathrm{Im}[\tilde{f}_{CM}]|\tilde{\mathbf{E}}|^2}{2\eta}\xi \tag{14}$$

where $R_{ROT}(\omega)$ is the rotation rate and ξ is a scaling factor that is introduced to consider that neither the viscosity η nor the electric field strength are precisely known. A typical four-electrode configuration used for ROT experiments is shown in figure 5. Here the rotating electric field is generated by four sine waves in phase quadrature.

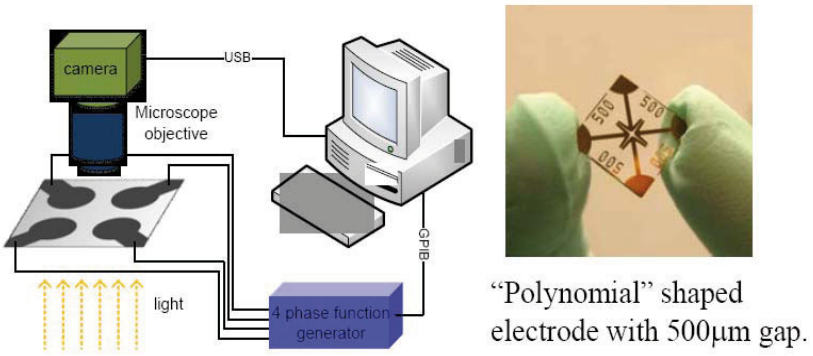

Figure 5. Diagram showing a typical set up of electrorotation (left) and an image of a chip for electrorotation (right).

The frequency spectra of both the DEP force and ROT torque (given by figure 2) can provide information on the dielectric properties of particles in suspension. The relationship between DEP and ROT can be examined using Argand diagrams (Wang et al., 1992, 1993), where the real and imaginary parts of the Clausius-Mossotti factor are mapped onto the complex plane as a function of frequency.

3 Micro-particle Manipulation

Micro-particles in suspension can be manipulated using DEP. The force depends on the magnitude of the field and the gradient, together with the particle volume. The direction of the force depends on the Clausius Mossotti factor, which is a measure of the polarisability of the particle in the suspending medium and importantly varies with the frequency of the applied potential (as shown in figure 2). Particle manipulation and separation have been achieved using a wide range of different electrode configurations. In this section, we review three classical electrode configurations that have been used for DEP manipulation: castellated electrodes, polynomial electrodes and interdigitated electrodes, the later used for field flow fraction (FFF) separation. We then describe recent applications of insulator-based DEP for particle sorting and the use of nDEP for single particle trapping.

3.1 Classical Electrode Configurations

A castellated electrode is shown in figure 6a. The electrodes are designed such that regions of the both positive and negative DEP can be found simultaneously. The array was first used by Pethig's group (Price et al., 1988; Burt et al., 1989) to dielectrophoretically collect particles. Typical electrode dimensions are 10 to 100 μm width and gap. The field is maximum at the electrode tips and minimum in the gaps between electrodes as shown in the figure 6b. This electrode array has been widely used both to separate and to characterize the DEP behavior of particles. Particle experiencing pDEP collect on the tips, and those experiencing nDEP in the gaps.

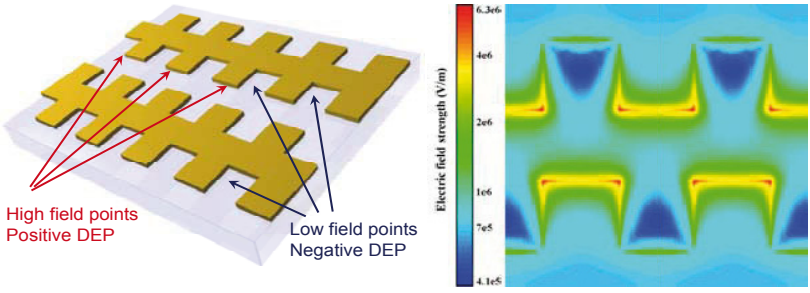

Figure 6. Schematic diagram of a castellated electrode, where typical electrode gap and spacing is 10 μm to 100 μm (left) and (b) an electric field plot showing the high field regions at the electrode tips.

The polynomial electrode design is shown figure 7 and has four electrodes arranged around a centre point, with the edges defined by a hyperbolic function in the centre, with parallel edges out to an arbitrary distance. The principle underlying this electrode design has been described by Huang et al. (1992). In the centre there is a region of almost uniform field gradient; particles can be trapped here by nDEP. At the electrode edges the field gradient is maximum. The polynomial electrode has been used for trapping and characterising a range of biological particles and also nano-particles (Green et al., 2000).

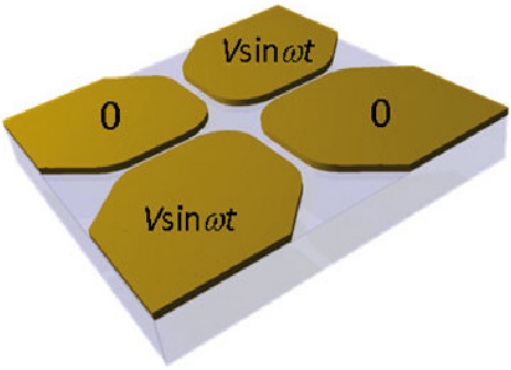

Figure 7. Schematic image of an electrode array defined by a polynomial, used for trapping cells in the centre by negative DEP.

The interdigitated electrode array (figure 8) is often used in DEP separation systems, since it generates a DEP force that decays exponentially from the surface. Depending on the applied frequency, the force either pulls particles towards the electrode edges or pushes particles away under nDEP.

When configured appropriately, this electrode array can also be used for twDEP. Here four AC signals phase shifted by 90^{o} are sequentially applied to the electrodes.

A knowledge of the electric field and field gradient is required to analyse and predict the behavior of particles in these electrode systems. The simplest electrode array is the interdigitated device (figure 8), and the electric field for this system can be determined in a number of ways, including using numerical methods or analytical approaches such as Schwarz-Christoffel Mapping (Sun et al., 2007). In this paper, full analytical solutions were given for the electric field, the dielectrophoretic and travelling-wave dielectrophoretic forces for the interdigitated electrode arrays.

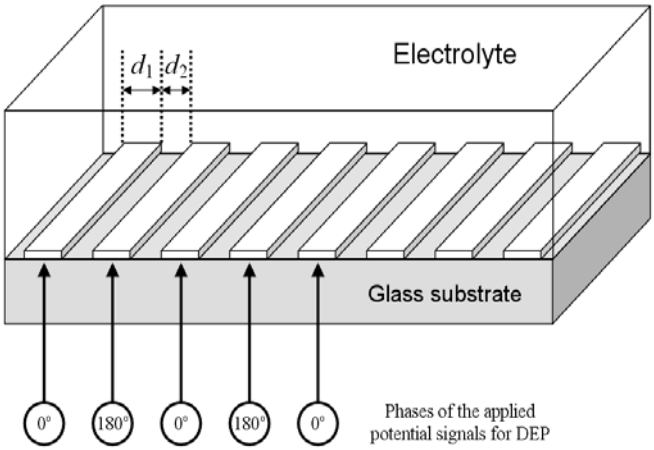

Figure 8. Schematic diagram of an interdigitated electrode array used for DEP (as in the diagram) or also for travelling wave DEP, where the electrodes are addressed by four phase shifted sine waves.

The interdigitated electrode array has been used to develop a DEP based separation system. Using a technique called Field Flow Fraction (FFF) (Rousselet et al., 1998; Gascoyne and Vykoukal, 2004) a deterministic force is combined with a fluid flow to provide a method for particle fractionation. Figure 9 shows a DEP-FFF system. Particles are introduced into the system and when the electric field is switched on, they experience a nDEP which pushes them up and away from the electrodes. This forces is balanced by a downward acting gravitational (buoyancy) force.

Depending on a combination of volume, mass density and polarisability, different particles move to different equilibrium positions in the system. When a laminar flow is applied, the fluid carries particles out of the device at a rate that depends on their original equilibrium position. Since different types of the particles are transported at different rates, a heterogeneous sample can be separated and fractionated along the channel. Recent examples of this technique include device for separating complex mixtures of different blood cells.

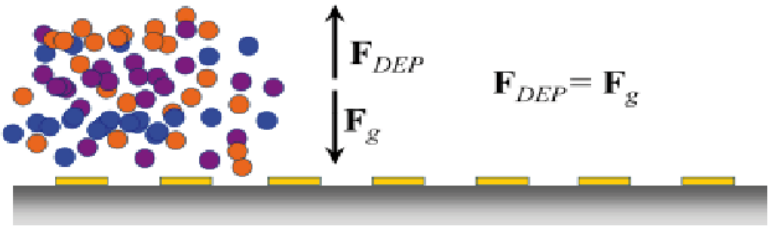

Figure 9. Diagram showing the principle of hyper-layer DEP FFF system. Particles are separated in the vertical direction by a balance of nDEP and gravitational forces. A parabolic fluid flow is applied and particles are fractionated.

3.2 Insulator-based DEP

Dielectrophoresis does not always have to be performed with conducting metal electrodes. The electric field can be modulated using insulating structures placed within a conducting electrolyte fluid. 3D insulating-post arrays (Lapizco-Encinas et al., 2004a,b) have been used to trap and separate live and dead bacteria. In this case large DC voltages are applied across the length of a microchannel. The insulating posts in the channel create obstructions in the pathways of the electric field producing non-uniformities in the electric field distribution in the channel, causing particle DEP. A continuous-flow dielectrophoretic spectrometer system has also been developed based on an insulating DEP technique using 3D geometries (Hawkins et al., 2007). Different field gradients were generated within a structure by fabricating devices with constrictions in a channel as shown in figure 10. These constriction in depth create regions of different field gradient. The device is able to continuously separate particles, as shown in figure 10.

3.3 Single cell trapping

Single cell trapping is important in many applications of biotechnology, such as the study of cell-cell interaction, drug screening and diagnostics. Cells can be trapped at regions of high electric fields (electrode edges or tips) by pDEP, but this requires that the cells are re-suspended in a low conductivity buffer (see figure 3). When cells are suspended in a high conductivity physiological buffer, they only experience nDEP. Electric field

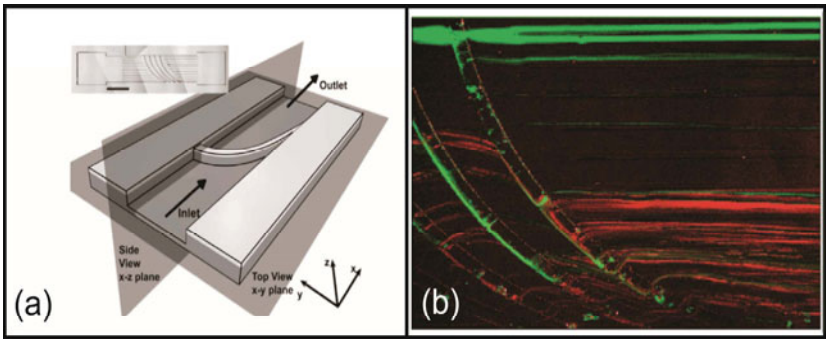

Figure 10. (a) Schematic showing the insulating-post geometry, which incorporates a curved constriction in the channel depth (b) Image showing separation of 2 μm (pseudo-colored green) and 3 μm particles (pseudo-colored red). The 2 μm particles pass the ridge without deflection, while the 3 μm particles are deflected due to higher DEP mobility. Reprinted with permission from (Hawkins et al. 2007), © 2007 American Chemical Society.

cages that generate nDEP forces to trap single cells were first introduced by Fuhr et al. (1992). Since then single cell trapping systems have been widely studied. Müller et al. (1996) used planar quadrupole electrode configuration to trap and concentrate micrometer and sub-micrometer particles. A 3-D microelectrode system (Müller et al., 1999) consisting of two layers of electrode structures was designed to focus, trap and separate cells and latex beads using nDEP. Schnelle et al. (1999, 2000) fabricated an AC cage with octode electrode to trap cells against a fluid stream. Voldman et al. (2001, 2002) and Voldman (2003) developed multiple single cell DEP traps, and a review of cell manipulation technologies based on DEP forces has been published by Voldman (2006). Various electrode geometries such as the quadrupole and octopole electrode, nDEP microwells, point-and-lid geometry and ring-dot geometry were described and evaluated.

A novel design of particle trap that uses nDEP (Thomas et al., 2009) is shown in figure 11. The array of single cell trap consists of a metal ring electrode and a surrounding ground plane - figure 11a. This ring electrodes creates a closed electric field cage in the centre (figure 11) and can be used to trap single cells, using "one wire per trap". Figure 11c shows 15 μm diameter beads trapped against. The behavior of the trap as a function of the fluid flow has been characterized (Thomas et al., 2009).

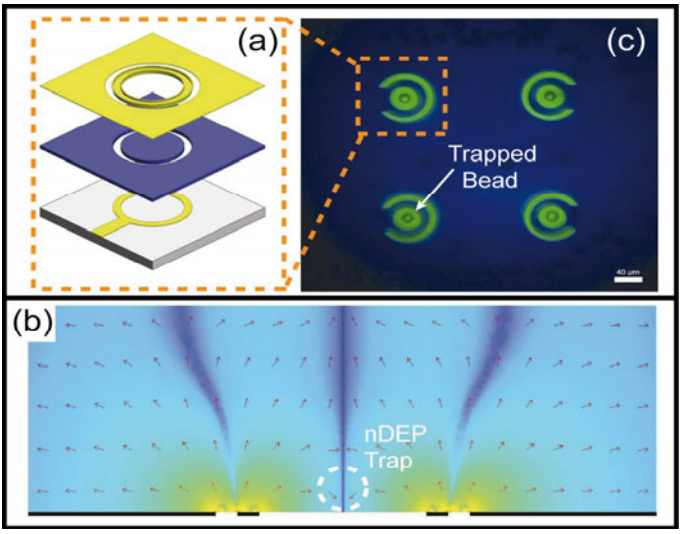

Figure 11. (a) Diagram showing the structure of a ring electrode. (b) Numerical simulation showing DEP force vectors and electric field distribution in the ring trap. (c) Four 40 μm diameter ring traps from an array of 48 traps. Single beads are captured by nDEP. Reprinted with permission from (Thomas et al., 2009), © 2009 Royal Society of Chemistry.

4 Micro-particle Characterization

4.1 Particle characterization

Apart from manipulating particles, DEP has also been used to characterize the dielectric properties of particles. Since the dielectrophoretic force is proportional to the effective polarisability (Clausius-Mossotti factor) of the particle, measurement of the force on a particle can be directly used to determine the permittivity and conductivity of the particle. In practice, it is difficult to measure the dielectrophoretic force on a particle from many reasons, including the effect of electrically induced fluid flow, interaction of a particle with a surface, or Brownian motion for small particles. An alternative is to measure the frequency at which the DEP is zero, or the cross-over frequency (Green and Morgan, 1999; Hughes and Morgan, 1999; Ermolina and Morgan, 2005; Jones, 1995). At this frequency, the real part of the particle polarisability is the same as the suspending medium and the dielectrophoretic force is zero. This point can be measured as a function of

medium conductivity and provides sufficient information to determine the dielectric properties of the suspended particles. This type of measurements involves observing the motion of single particles experiencing DEP using a fluorescence microscope. Depending on the applied frequency, particles move either towards an electrode under positive DEP or away from an electrode under negative DEP. At a particular frequency (or frequencies) the DEP force is zero and the particle will remain stationary, i.e. when $\mathrm{Re}[\tilde{f}_{CM}] = 0$. If the properties of the suspending fluid are known, then the effective complex permittivity of the particle can be calculated. According to equation 10, the crossover frequency is defined to be the frequency point that the real part of the Clausius-Mossotti factor equals zero;

$$f_{cross} = \frac{1}{\sqrt{2\pi}} \sqrt{\frac{\sigma_m - \sigma_p}{\epsilon_p - \epsilon_m} f_{MW}} \tag{15}$$

with

$$f_{MW} = \frac{1}{2\pi\tau_{MW}} \tag{16}$$

$$\tau_{MW} = \frac{\epsilon_p + 2\epsilon_m}{\sigma_p + 2\sigma_m} \tag{17}$$

where f_{cross} is the cross-over frequency, f_{MW} is the Maxwell-Wagner relaxation frequency and τ_{MW} is the Maxwell-Wagner time constant of the relaxation.

In a typical experiment, the zero force or cross-over frequency is measured for different suspending medium conductivities spanning two to three decades. For a solid homogeneous spherical particle, a frequency vs. conductivity map can be plotted as shown in figure 12. For frequencies and conductivities corresponding to the shaded area only positive DEP is observed. For all other regions, for example at high conductivities when the particle's effective polarisability is always less than the suspending medium, only negative DEP is observed.

Recently, an evolution of zero force characterization has been developed, called iso-dielectric separation (IDS) technology (Vahey and Voldman, 2009), as shown in figure 13. In this methodology, particles are dielectrophoretically concentrated to a region along an electrical conductivity gradient where the effective polarisability of particles goes to zero. By measuring this isodielectric position and operating with an appropriate frequency and amplitude of the applied voltage, a mixture of particles and cells can be separated and simultaneously characterized.

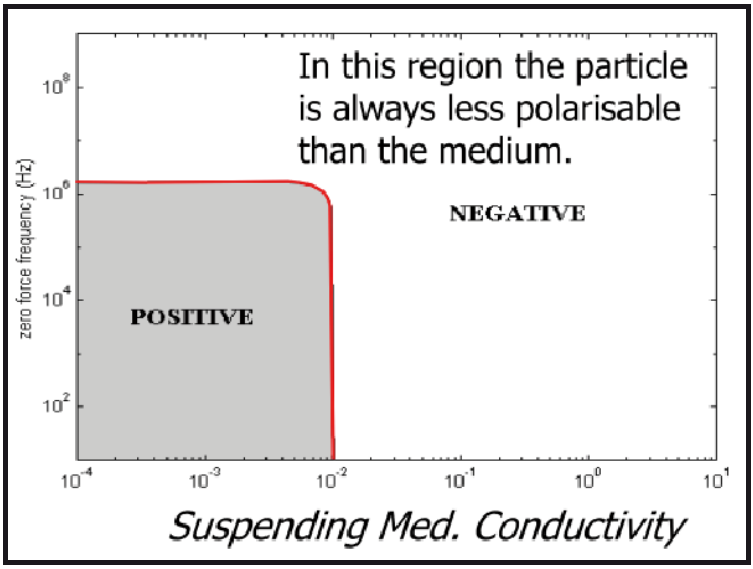

Figure 12. A plot showing the zero force point (cross-over frequency) varies with suspending medium conductivity for a 557 nm diameter particle with relative permittivity 2.55 and conductivity 10 mSm^{-1}.

4.2 DEP for microfluidic systems

Many biomedical and diagnostic applications require fast and accurate analysis of single particles. For example, blood contains many types of cell that can be discriminated on the basis of their optical and/or electrical properties. Morgan et al. (2006) designed and built a device to measure both the optical and electrical-impedance properties of cells at high speed using a microfabricated cytometer. For efficient and high-speed characterization of single particles, the particles need to be focused into the centre of a fluid stream. This can be accomplished using DEP, as shown in figures 14 (a) and (b), where four thin (100 nm) electrodes are fabricated on the base and lid of a microchannel (Holmes et al., 2006). Using a high frequency (20MHz) voltage, the electric field generated by the electrodes produces nDEP force onto the particles pushing particles away from the electrode edges. As the gap between the electrodes decreases, the particles are gradually forced into a narrow focused beam, in which single particles are well aligned, as demonstrated in figure 14 (c).

In this way the properties of the single particles can be measured using

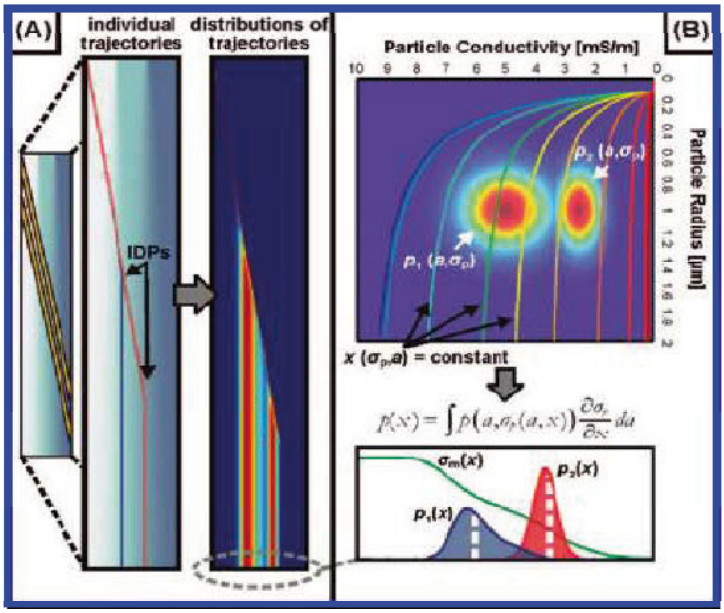

Figure 13. Particles with different electrical properties (i.e. conductivity) go along with different trajectories in an electrical conductivity gradient environment under DEP. Reprinted with permission from (Vahey and Voldman, 2009), © 2009 American Chemical Society.

fluorescence spectroscopy or electrical impedance spectroscopy, as shown in figure 15a. Particles pass through a laser and scatter light: the amount of scatter depends on particle size and shape. Particles can also be labeled with fluorescent antibodies that emit light when excited by the laser. Simultaneously, the electrical impedance of single particles can be measured. This is done by fabricating chips with microelectrodes precisely positioned in the microchannel. The electrodes are a similar size to a particle (typically 10 μm to 20 μm wide, with similar gaps) and are energized with an AC signal of a few hundred millivolts. Particles flow through the impedance detection region, confined by the microelectrodes, one at a time, so that sensitive circuitry can determine the electrical properties of single cells (Morgan et al., 2007). This type of impedance spectroscopy can discriminate between cells without resorting to labeling. Figure 15b shows the simultaneously measured fluorescent signal and impedance signal of a 5.49 μm bead, while a higher impedance amplitude signal of a 7.18 μm bead is also captured.

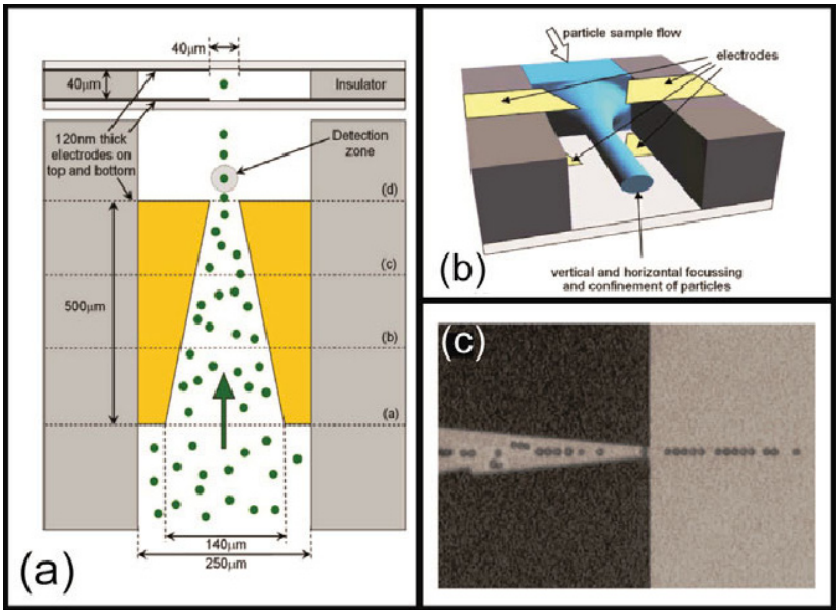

Figure 14. (a) Schematic showing the four focusing electrodes in top-down and cross-sectional view. (b)Diagram showing the principle of 3D dielectrophoretic focusing. (c) Photograph showing the focusing of 6 μm diameter latex beads. Reprinted with permission from (Holmes et al., 2006), © 2006 Elsevier.

A challenge in single particle impedance analysis was to develop a way of measuring a broad band of frequencies at once, in the time it takes a particle to pass through the detection zone. This has been resolved by exciting the cells using a pseudo-random binary signal, maximum length sequences. Impedance data of single particle distributed at 512 frequencies can be measured within 1 ms (Sun et al., 2007a,b).

5 Nanoscale DEP

The forces acting on particles in suspension can be categorized as stochastic, i.e. Brownian motion, and deterministic, such as viscous drag, gravitational or dielectrophoretic. When an electric field is applied to a fluid there are other electric-field induced forces (electrohydrodynamic) in the systems. The Brownian motion of a particle arises from the thermal energy of the

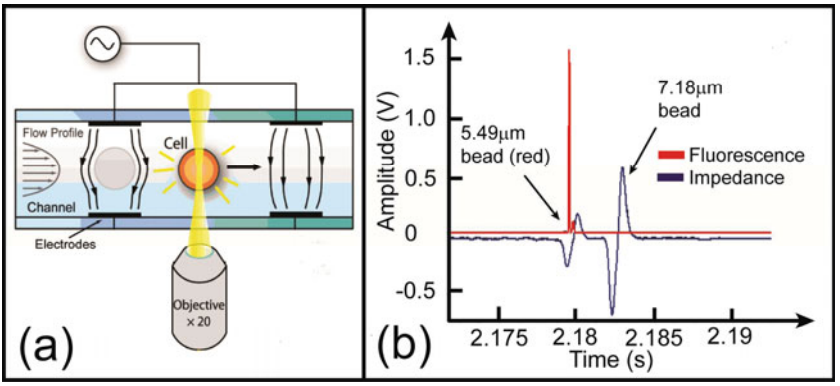

Figure 15. (a) Diagram showing the simultaneously optical and electrical characterization for single particle analysis in a microchip. (b) Plot showing the fluorescent and impedance signal of a single 5.49 μm bead. The 7.18 μm has no fluorescent signal but displays higher impedance amplitude.

system, which causes the particles to move in a random way. There is very little that can be done to control Brownian motion, other than cooling or increasing the viscosity of the liquid. In contrast to stochastic force, the deterministic forces are not random and can be controlled.

5.1 Navier-Stoke's equation and the Stoke's drag force

The Navier-Stokes equation is the equation of motion for the fluid and is derived from conservation of momentum arguments. For an incompressible Newtonian fluid, the Navier-Stokes equation is:

$$\rho_m \frac{\partial \mathbf{u}}{\partial t} + \rho_m(\mathbf{u}\cdot\nabla)\mathbf{u} = -\nabla p + \eta\nabla^2\mathbf{u} + \mathbf{f} \tag{18}$$

where ρ_m is the mass density, $\mathbf{u}$ is the velocity of the fluid, t is time, p is the pressure, η is the viscosity and $\mathbf{f}$ is the total applied force (force per unit volume) acting on the fluid.

The ratio of the inertial term, $\rho_m(\mathbf{u}\cdot\nabla)\mathbf{u}$, to the viscous term, $\eta\nabla^2\mathbf{u}$ is the Reynolds number (Re), a parameter that is used to characterize microfluidic systems:

$$\mathrm{Re} = \frac{\rho_m u_0 l_0}{\eta} \tag{19}$$

with l_0 a length scale and u_0 a typical velocity. For low values of Reynolds number (Re$\ll$ 1) the viscous term dominates, whilst for high values (Re$\gg$ 1)

the inertial term dominates. In microfluidic systems, microfabricated channels and chambers are used to guide the fluid through the device. Typical dimensions for these channels vary between $10\,\mu$m and 1 mm. The flow in such channels is generally laminar i.e. the fluid flow follows streamlines and is free of turbulence.

For a particle moving in the fluid, the fluid exerts a drag force on the particle that affects the velocity of the particle. The force is known as the Stokes force

$$\mathbf{F}_\eta = -f\mathbf{u} \tag{20}$$

where the constant f is the friction factor, a factor that depends on particle parameters such as size, shape and surface characteristics. For a spherical particle of radius R, the Stokes force is given by:

$$\mathbf{F}_\eta = -6\pi\eta R\mathbf{u} \tag{21}$$

5.2 Gravitational force

For a particle with a mass density of ρ_p, suspended in a medium with density of ρ_m, the effective mass of the particle is equal to the volume of the particle times the difference in mass densities between the particle and the suspending medium. In a gravitational field, the magnitude of the gravitational force, $\mathbf{F}_g$ is given by:

$$\mathbf{F}_g = \frac{4}{3}\pi R^3(\rho_p - \rho_m)\mathbf{g} \tag{22}$$

where $\mathbf{g}$ is the gravitational acceleration.

The gravitational force is counteracted by the Stoke's drag force, therefore substitute equation 21 into 22 to give the sedimentation velocity of the particle:

$$u_g = \frac{2}{9}\frac{R^2(\rho_p - \rho_m)g}{\eta} \tag{23}$$

The magnitude of this velocity is variable, for example a 500 nm latex sphere has a mass density of 1050 kg/m^3 giving a sedimentation velocity of only 7 nm/s, indicating the particle moves a distance of the order of its diameter in a minute. However, for a cell, which is much greater, the sedimentation velocity can approach 1 to 10 μm/s in water. Although the gravitational forces acting on sub-micron particles are small, they are not insignificant and cannot always be ignored.

5.3 Electric field induced forces (electrohydrodynamics)

There are two major forces that can be induced through the interaction of the applied electric field with the fluid. The first is the electrothermal

force, which is due to the interaction between the electric field and the gradients of the dielectric properties (permittivity and conductivity) of the fluid. These gradients in dielectric properties are generally caused by heating of the fluid, either directly from the electric field (Joule heating) or from some other external sources. This interaction gives rise to an electrothermal body force (Ramos et al., 1998). A second force is due to the interaction between the applied electric field and the induced free charges in the electrical double layer between the electrode and the electrolyte, which causes the fluid to move, a flow called AC electroosmosis (Ramos et al., 1998). At low frequencies, the potential applied to a metal electrode causes charge accumulation in the electrode-electrolyte double layer. In AC electrokinetics, the difference between electrothermal flow and AC electroosmosis is generally observed in the frequency domain. At low frequencies (< 100 kHz), AC electroosmosis dominates the fluid flow. As the frequency increases, this flow diminishes so that above 100 kHz, the behavior of the fluid is dominated by electrothermal force. However, the latter force is only substantial if there is significant temperature gradients in the fluid, for example due to Joule heating in a fluid of high electrical conductivity. Detailed descriptions on electrothermal and electroosmotic effects can be found elsewhere (Ramos et al., 1998; Castellanos et al., 2003; Morgan and Green, 2003).

5.4 Scaling laws

In order to move particles in a deterministic manner a knowledge of the forces acting on the particles is required. Importantly, the displacement due to the deterministic force should dominate over the random or stochastic force. The two main forces that act on particles in addition to DEP are gravitational and Brownian motion. The relative scale of these forces is often difficult to determine, but can be evaluated analytically for some simple geometries. In particular one of the easiest geometries is a semi-infinite parallel plate structure, consisting of two coplanar rectangular electrodes with an infinitely small gap, as shown in figure 16a (Castellanos et al., 2003). In this geometry, the field as a function of radial distance (r) is $E = V/r$, where V is the amplitude of the applied voltage and r is the distance to the centre of the gap. The influence of Brownian motion, gravity and DEP on a single particle can be calculated for this electrode structure, and the results are summarized in figure 16b (Castellanos et al., 2003). This plot shows the displacement of a particle during a time interval of one second as a function of particle radius, R. For an electrode gap of $25\,\mu$m, and with an applied potential of 5 volts, it can be seen that the displacement due to Brownian motion is greater than that due to DEP for a particle

less than 0.4 μm diameter. Also, gravity is less important than DEP for any particle sizes, since both scale as R^2. The deterministic manipulation of particles smaller than 0.4 μm can be achieved if the magnitude of the applied voltage is increased, or the characteristic length of the system r is reduced. One simple scaling law comes from the relationship between field gradient and electrode gap. For example, reducing the electrode gap by one order of magnitude increases the DEP force by three orders of magnitude. Although figure 16b shows that it is relatively easy to move small particles simply by increasing the electric field, this assertion assumes that there are no other forces. This is generally not the case, since depending on the frequency and the conductivity of the suspending medium there is often an electrohydrodynamic force on the fluid.

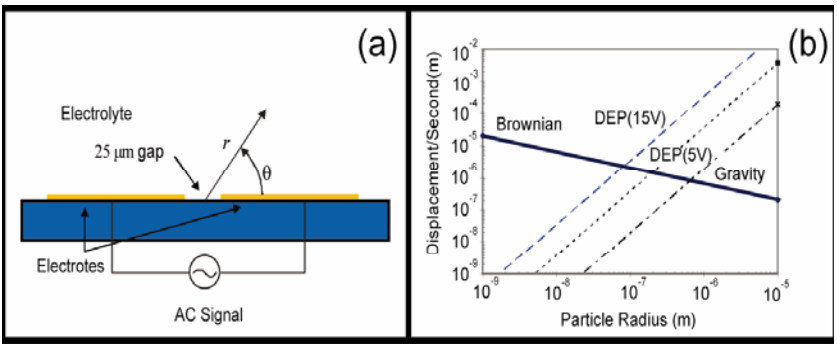

Figure 16. (a) Simple electrode geometry consisting of two parallel plate electrodes with a small gap used to calculate the typical particle displacements. (b) Particle displacement in one second versus particle radius for a particle of mass density 1050 kgm^{-3}. The characteristic length used in this figure is $r = 25$ μm. Reprinted with permission from (Castellanos et al., 2003), © Institute of Physics.

5.5 Nano-particle separation

Polymer particles do not behave as perfect insulators. They have a net surface charge density and are characterized by a surface conductance. Charges move along the surface, giving rise to a surface conductance, K_s, which is related to an equivalent bulk conductivity of the particle through:

$$\sigma_p = 2K_s/R \tag{24}$$

According to this equation, surface conductance plays a significant role in determining the conductivity in small sized ($< 1\mu$m) particles since it is inversely proportional to particle radius. At low frequencies, small polystyrene particles are generally more polarisable than the suspending medium and experience pDEP. At high frequencies, the properties of the system are dominated by permittivity, the particles have a much lower permittivity that water, they are less polarisable and therefore experience nDEP. Separation of sub-micrometre particles can be achieved in a number of ways, and was demonstrated using electrodes such as castellated or polynomial (Green et al., 2000). Apart from size-based separation, a mixture of the same size particles can be separated because of differences in surface charge densities, as given by equation 24.

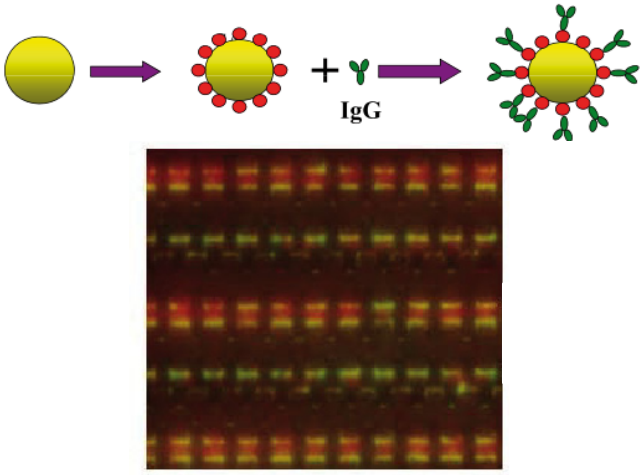

Figure 17. Schematic of surface-modified latex particles (above) and photograph (below) showing separation of unmodified and protein conjugated 216 nm diameter latex particles due to positive DEP forces of different magnitude. The protein-conjugated beads form pearl chains between the tips of the castellated electrode array. The unmodified particles (brighter in the picture) experience a significantly stronger positive DEP force and are attracted to the electrode tips. Reprinted with permission from (Morgan et al., 1999), © 1999 Elsevier.

One method of differentiating the same sized particles is to modify their